Macromolecules

pubs.acs.org/Macromolecules Article

Polyolefin Ionomer Synthesis Enabled by C−H Thioheteroarylation

Quan H. Tran, Eliza K. Neidhart, Sergei S. Sheiko, Wim Bras, and Frank A. Leibfarth*

Cite This: *Macromolecules* 2023, 56, 8920−8927 Read Online

ACCESS | Metrics & More | Article Recommendations | Supporting Information

ABSTRACT: Chemical upcycling of plastic waste into high-value materials has the potential to contribute to a more sustainable plastic economy. We report the synthesis of high-value ionomers directly from commodity polyolefins enabled by amidyl radical-mediated C−H functionalization. The use of thiosulfonates as a linchpin functionality for the group transfer of a variety of heteroaryl groups provided tunable incorporation of ionizable functionality onto a variety of polyolefin substrates, including postconsumer polyethylene packaging waste. Synthetic, structural, and thermomechanical studies provided a comprehensive understanding of both structure−reactivity and structure−property relationships for polyolefin ionomers. X-ray scattering experiments conducted in the solid and melt states confirm the presence of ionic multiplets that serve as physical cross-links both below and above the melting temperature of polyolefin crystallites. The incorporation of ionic groups into the polyolefins yielded materials with significantly enhanced melt strength and tensile toughness. We anticipate that this approach to access performance-advantaged polyolefin ionomers from commodity substrates or plastic waste will enhance sustainability efforts and lead to new opportunities for this versatile class of thermoplastics.

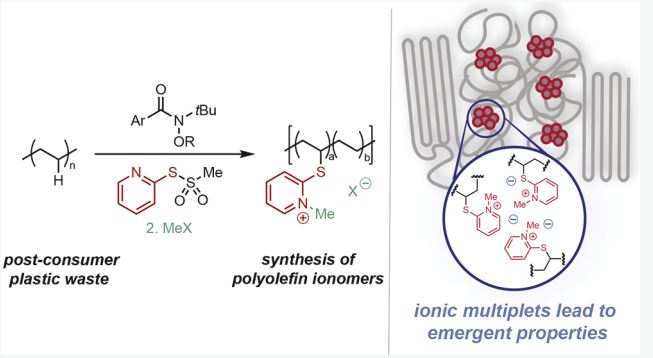

INTRODUCTION

Polyolefins comprised nearly 50% of polymer production in 2021.[1] The low cost, chemical stability, and beneficial thermomechanical properties of polyolefins make them useful for a variety of single-use applications in packaging, construction materials, and automotive components, among others.[2] While polyolefins are ubiquitous, the poor recycling rate (<5%) and leakage of waste into the environment present acute societal and environmental challenges.[3−5] Furthermore, limitations in sorting technologies at material recovery facilities often result in mixtures of polyolefins, additives, and impurities, which result in a substantial deterioration in properties after mechanical reprocessing.[5−7] Upcycling, or chemical reactions that transform plastic waste into products with increased value, is an emerging concept that could improve plastic waste management.[8,9] The high bond dissociation energies (BDEs) of aliphatic C−H bonds, however, make the selective functionalization or deconstruction of polyolefins challenging.[10,11]

Polyolefin ionomers are a high-value class of materials composed of a hydrocarbon backbone that contains a relatively low concentration (<15 mol %) of ionic groups.[12−14] Due to the mismatch between the nonpolar polymer backbone and the polar ionic groups, polyolefin ionomers exhibit microphase separation into ion-rich domains dispersed within a nonpolar polymer matrix.[15−17] These ionic domains, referred to as multiplets by Eisenberg et al.,[18] behave as physical cross-links and imbue the material with high impact strength, improved abrasion resistance, enhanced optical clarity, and increased toughness compared to their polyolefin counterparts.[19−21] DuPont commercialized polyolefin ionomers in the 1960s under the trade name Surlyn, and these materials are currently sold by Dow for high-end packaging, medical, and sports applications.[22,23] Surlyn ionomers are synthesized through the free radical copolymerization of ethylene and (meth)acrylic acid, followed by neutralization of the carboxylic acids with alkali metals or zinc to provide the ionomer (Figure 1A). This energy-intensive polymerization process requires high pressures (1,000 to 3,000 atm of ethylene), precludes the use of α-olefins as comonomers, results in exclusively a highly branched low-density polyethylene-like microstructure, and limits ionic group identity to a carboxylate.[24]

To overcome the limitations of radical copolymerization to access polyolefin ionomers, a number of transition-metal-catalyzed copolymerization methods have been reported. The use of industrially relevant catalysts that proceed through coordinative processes can copolymerize ethylene and α-olefins with functionality that can be ionized post-polymerization. Chung and co-workers demonstrated that silane-

Received: August 11, 2023
Revised: September 24, 2023
Published: October 19, 2023

https://doi.org/10.1021/acs.macromol.3c01610
Macromolecules 2023, 56, 8920−8927

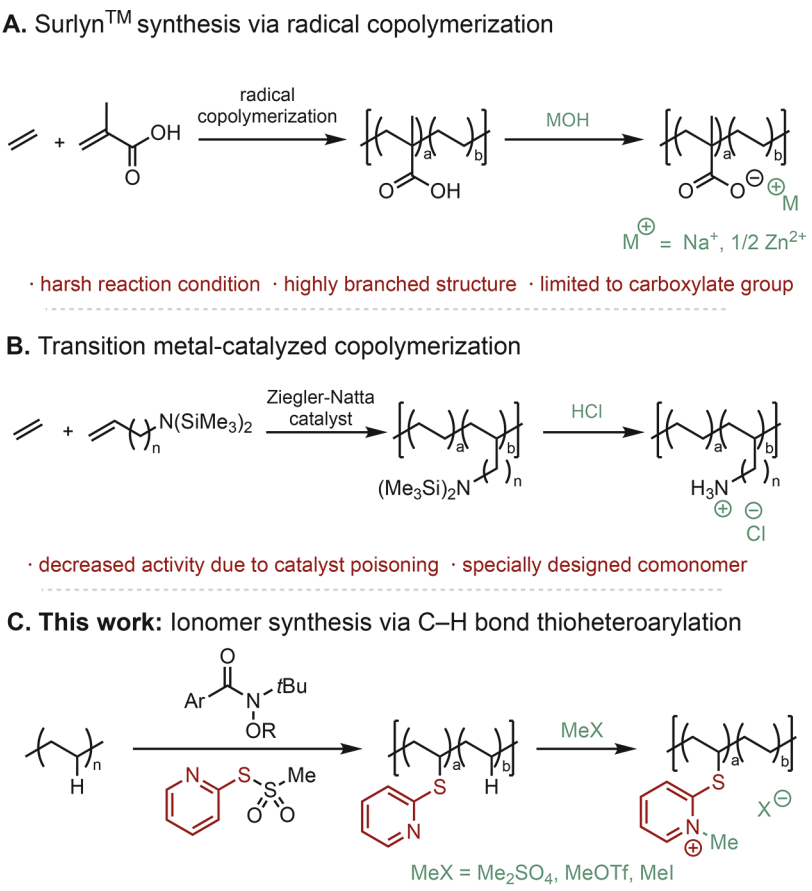

Figure 1. Approaches to synthesize polyolefin ionomers. (A) Radical copolymerization of ethylene and (meth)acrylic acid is commercially practiced. (B) Transition-metal-catalyzed copolymerization and subsequent modification. (C) This work serves as a complementary approach by synthesizing polyolefin ionomers from commodity polyolefins or plastic waste through C−H functionalization.

protected amino-α-olefin comonomers could be copolymerized with ethylene or propylene, where the sterically encumbered silyl protecting groups minimized poisoning of the zirconium metallocene catalyst.[25,26] Deprotection of the silyl protecting groups yielded primary amine-containing copolymers, which could be protonated to yield ammonium polyolefin ionomers (Figure 1B). An alternative approach was recently reported by Lopez-Barron et al., wherein copolymerization of a trialkyl aluminum-containing monomer with propylene using a zirconium metallocene and subsequent oxidation to the aluminum carboxylate provided an isotactic polypropylene ionomer.[27,28] The incorporation of low comonomer content (<0.1 mol %) resulted in materials with similar crystallinity, melting point, and mechanical properties of the iPP homopolymer while also demonstrating improved melt strength and shear-thinning properties. While these approaches are attractive, they require the synthesis of specialty monomers and/or ligands and result in diminished catalyst activities.

To expand the range of synthetic approaches, late transition metal catalysts have been explored that are more tolerant to functional comonomers. Ye et al. reported the synthesis of tetraalkylammonium-containing polyethylene ionomers through Pd-catalyzed copolymerization of ethylene with an acrylic tetraalkylammonium comonomer.[29] While this elegant example demonstrates the possibility of direct copolymerization, the polar comonomer significantly reduced the catalyst efficiency and produced a highly branched microstructure. Alternatively, metathesis polymerization using Grubbs's ruthenium catalysts has been successful in producing a variety of polyolefin ionomers. For example, Wagener and co-workers have used acyclic diene metathesis (ADMET) polymerization to produce imidazolium, carboxylate, and sulfonate-containing polyolefin ionomers, in which each ionic group is precisely spaced along the polymer chain.[30−33]

An alternative but rarely considered approach to polyolefin ionomers is to place ionic functionality onto a polyolefin postpolymerization, which would enable the use of commodity polyolefin or plastic waste as a starting material to access this high-value product. Previously, C−H functionalization of high-density polyethylene (HDPE) or isotactic polypropylene (iPP) using peroxides as hydrogen atom transfer (HAT) reagents has furnished anhydride-functionalized polyolefins, which could subsequently be reacted with nucleophiles to access polyolefin ionomers.[34−36] The lack of selectivity for HAT using peroxides results in β-scission and long-chain branching of polyolefins, which adversely affects their molecular weight distribution and complicates quantitative structure−property evaluation.[10,37] Recently, our group reported an *O*-alkenylhydroxamate reagent that, upon thermolysis, provides regioselective HAT, followed by functional group transfer to a variety of linear and branched polyolefin substrates, including postconsumer plastic waste.[38] To demonstrate the unique advantages provided by this approach, we installed a primary alkyl halide onto linear low-density polyethylene (LLDPE) and subsequently generated an imidazolium polyolefin ionomer by displacement of the halide

https://doi.org/10.1021/acs.macromol.3c01610
Macromolecules 2023, 56, 8920−8927

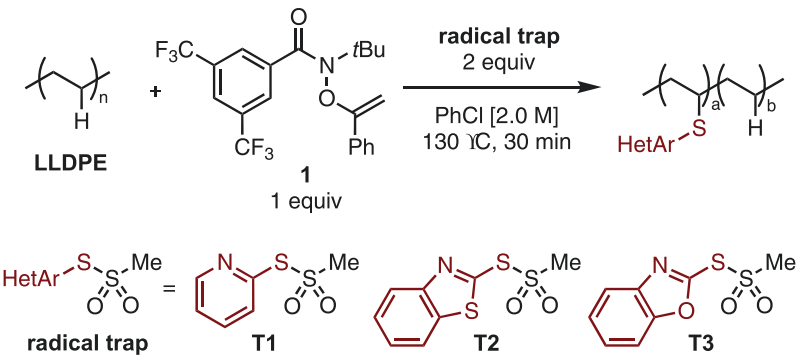

Polymer	Radical trap	Ratio of **1** relative to r.u.[a]	mol% func.[b]	M_n[c] kg/mol	$Đ$[c]
P1 (1.3-Pyr-LLDPE)	**T1**	1:50	1.3	19	3.6
P2 (3.1-Pyr-LLDPE)	**T1**	1:20	3.1	20	4.1
P3 (5.9-Pyr-LLDPE)	**T1**	1:10	5.9	19	3.3
P4 (3.0-Bt-LLDPE)	**T2**	1:20	3.0	20	3.6
P5 (3.3-Bx-LLDPE)	**T3**	1:20	3.3	22	3.6
P6[d] (1.3-Pyr-HDPE)	**T1**	1:50	1.3	33	4.1
P7[e] (1.3-Pyr-LDPE)	**T1**	1:50	1.3	41	8.9
P8[f] (1.0-Pyr-PCPE)	**T1**	1:50	1.0	38	6.2
P9[g] (0.6-Pyr-iPP)	**T1**	1:50	0.6	69	4.9

Figure 2. Thioheteroarylation of polyolefins through amidyl radical-mediated C−H functionalization provides polyolefins with diverse heteroaryl functionalities; standard conditions: LLDPE (M_n = 21 kg/mol, $Đ$ = 3.8), **1**, radical trap, PhCl (2.0 M), 130 °C, 30 min. [a] r.u. = repeat unit. [b] mol % functionalization determined by ^{1}H NMR in $C_2D_2Cl_4$ at 110 °C. [c] Molar mass and dispersity was determined by GPC in 1,2,4-trichlorobenzene at 140 °C. [d] HDPE (M_n = 35 kg/mol, $Đ$ = 4.0) was used. [e] LDPE (M_n = 34 kg/mol, $Đ$ = 13.5) was used. [f] PCPE (M_n = 34 kg/mol, $Đ$ = 7.8) was used. [g] iPP (M_n = 62 kg/mol, $Đ$ = 5.1) was used.

with methyl imidazole. The tensile properties of the imidazolium ionomer were similar to a sample of Surlyn, demonstrating that our post-polymerization modification approach could produce a material with functional equivalence to high-value commercial ionomers. While this approach served as a valuable proof-of-concept for upcycling polyolefins into a polyolefin ionomer, the ion identity was limited to an imidazolium and the postpolymerization reaction of the alkyl halide was inefficient. We hypothesized that alternative radical traps would provide a more versatile and efficient method to access a broader range of polyolefin ionomers via postpolymerization modification.

Herein, we report the synthesis and structure−property evaluation of a range of polyolefin ionomers through chemoselective C−H functionalization. Our approach leverages thiosulfonates as a versatile linchpin functionality for group transfer onto polyolefin substrates, which enables the addition of pyridyl, benzothiazolyl, and benzoxazolyl heteroarenes onto a variety of polyolefin substrates by using an *O*-alkenylhydroxamate reagent. Pyridyl-functionalized polyolefins could be quantitatively converted into pyridinium polyolefin ionomers (Figure 1C). A combination of structural and thermomechanical studies demonstrated that the pyridinium ions phase-separated into ionic multiplets, which served as physical cross-links both below and above the melting temperature of polyolefin crystallites.

RESULTS AND DISCUSSION

Thioheteroarylation of Polyolefins. We identified methanethiosulfonates as efficient group transfer reagents[39−41] to enable the introduction of diverse heteroaryl functional groups onto polyolefins. We hypothesized that the thiosulfonate would enable rapid radical trapping of polymer-centered radicals generated through amidyl radical-mediated HAT, while the sulfonyl radical byproduct would be selective for the reaction with the *O*-alkenylhydroxamate reagent (**1**) and would not participate in deleterious side reactions. Our studies commenced with the C−H thiopyridylation of LLDPE using **1** as an amidyl radical precursor and *S*-(pyridin-2-yl) methanesulfonothiolate (**T1**) as a radical trap. LLDPE was chosen as a model branched polyolefin substrate. Reacting LLDPE with reagent **1** and radical trap **T1** at a theoretical maximum functionalization of 2 mol % (i.e., 1 equiv of functional group per 50 repeat units) at 130 °C in chlorobenzene resulted in 1.3 mol % of polymer repeat units functionalized with pyridine, as measured by ^{1}H NMR spectroscopy (**P1**, Figure 2). Altering the stoichiometry of **1** and **T1** compared to the repeat unit enabled us to tune the areal density of heteroaryl groups on the polymer between 1.3 and 5.9 mol % (**P1**−**P3**, Figure 2).[42] Relatively low areal densities of functionalization were targeted in order to add a new function to the polyolefin while retaining the semicrystalline nature of the parent polymer.

To demonstrate the scope of this transformation, a variety of heteroaryl methanethiosulfonates were explored as radical trapping reagents. Benzothiazole and benzoxazole heteroarenes were competent for group transfer onto LLDPE and performed similarly to the pyridyl group (**P4** and **P5**, Figure 2). Regardless of the heteroarene-containing radical trap, the molar mass (M_n) and dispersity ($Đ$) were similar before and

https://doi.org/10.1021/acs.macromol.3c01610
Macromolecules 2023, 56, 8920−8927

after functionalization, as assessed by high-temperature gel permeation chromatography (GPC) (Figures 2 and S1). These data indicate a lack of deleterious chain scission or chain coupling. To expand the utility of this work beyond LLDPE, C−H thiopyridylation was successfully performed on complementary polyolefin substrates, including linear HDPE, highly branched LDPE, regularly branched iPP, and postconsumer waste PE (PCPE) obtained from foam packaging (**P6**−**P9**, Figures 2 and S2−S5). In addition to methanesulfonates, we also investigated the C−H thioheteroarylation using toluenethiosulfonate and disulfides as radical traps, which provided functionalized LLDPE, albeit at reduced efficiency (Table S1). The translational potential of this transformation was demonstrated by conducting C−H thioheteroarylation of LLDPE in a twin-screw extruder under solvent-free conditions. Physically mixing LLDPE, **1**, and **T1** at a theoretical maximum functionalization of 5.0 mol % in a conical twin-screw extruder for 3 min provided pyridyl-functionalized LLDPE with 1.4 mol % functionalization (**P10**, Table S1).

Synthesis of Polyolefin Ionomers. While the functionalization of polyolefins directly with an ionic group would be efficient, solubility challenges of ion-containing radical traps with the polymer precluded such an approach. Therefore, we hypothesized that quaternization of the nitrogen on the heteroarene could provide facile access to polyolefin ionomers. Reaction of electrophilic methylating reagents with benzothiazole- and benzoxazole-functionalized LLDPE led to inefficient quaternization, presumably due to the poor nucleophilicity of the heteroarenes. In contrast, the reaction of pyridyl-functionalized LLDPE with dimethyl sulfate led to full conversion into the pyridinium polyolefin ionomer (Figure 3). The ionomer

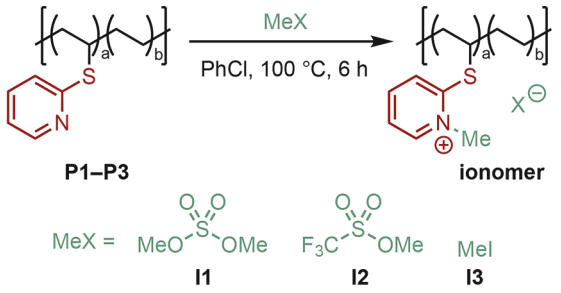

Ionomer	MeX	mol% func.	mol% ionic group[a]
P1-*ion*-S	**I1**	1.3	1.3
P2-*ion*-S	**I1**	3.0	3.0
P3-*ion*-S	**I1**	6.0	6.0
P1-*ion*-Tf	**I2**	1.3	1.3
P1-*ion*-I[b]	**I3**	1.3	1.0

Figure 3. Ionomer synthesis by reacting the pyridyl-functionalized LLDPE with electrophilic methylating reagents; synthetic conditions: Functionalized polymer, MeX (2 equiv compared to r.u.), PhCl (2.0 M), 100 °C, 6 h. [a] mol % ionic group determined by ^{1}H NMR in $C_2D_2Cl_4$ at 110 °C. [b] The reaction was conducted at 80 °C for 48 h.

with 1.3 mol % pyridinium sulfonate (**P1-*ion*-S**) was soluble in tetrachloroethane-d2 at 110 °C for ^{1}H NMR spectroscopy, which demonstrated the expected appearance of peaks for the product and complete disappearance of resonances for the starting polymer. The ionic content could be tuned in a range of 1.3−6.0 mol % by varying the mol % of pyridine on LLDPE, which showed that changing the stoichiometry of the initial functionalization reaction allows access to materials with systematically different amounts of ionic group incorporation. The solubility properties of the pyridinium ionomers were dependent on ion content; **P1-*ion*-S** with 1.3 mol % ionic functionalization is soluble in relatively low polarity solvents, such as tetrachloroethane, whereas **P2-*ion*-S** with 3.0 mol % functionalization is soluble in a 10:1 mixture of tetrachloroethane/dimethyl sulfoxide (DMSO) and **P3-*ion*-S** with 6.0 mol % functionalization is no longer soluble in tetrachloroethane and instead is only soluble in DMSO. Ionization with other quaternizing agents enabled access to polyolefin ionomers with different counteranions (Figure 3). Methylmethanesulfonate completely transformed pyridine-containing LLDPE into the pyridinium triflate-functionalized LLDPE (**P1-*ion*-Tf**), and methyl iodide gave a mixture of pyridyl- and pyridinium iodide-functionalized materials (**P1-*ion*-I**).

The thermal properties of the functionalized polyolefins were assessed to understand the structure−property relationships. The percent crystallinity (%) of the polymers was calculated from the enthalpies of melting in the second heating cycle of differential scanning calorimetry (DSC). We predicted that thiopyridylation of the polymer backbone would disrupt crystal packing and reduce the percent crystallinity. Unfunctionalized LLDPE exhibits a melting temperature (T_m) of 124 °C and a corresponding percent crystallinity of 41% (Figure 4B and Table S3). Pyridyl- and pyridinium-functionalized LLDPE bearing 1.3 mol % functional groups show melting temperatures of 112 and 110 °C, with percent crystallinity of 34% and 26%, respectively. Although the melting temperatures of materials are similar, the difference in their enthalpies of melting indicates that the transformation of the functionalized polymer into a polyolefin ionomer caused a

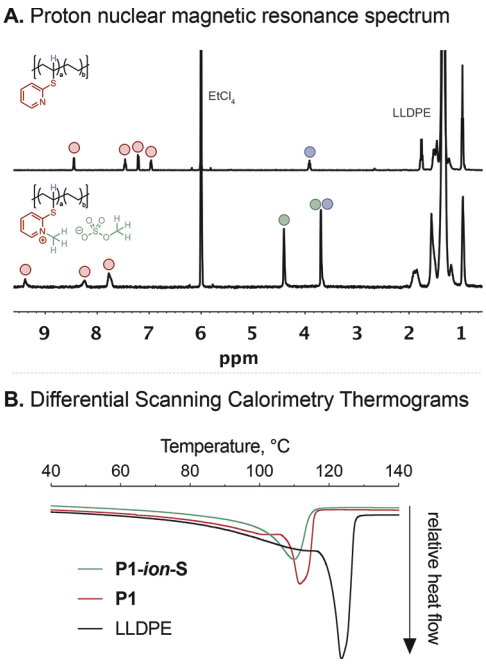

Figure 4. Chemical and thermal characterization of polyolefin ionomers. (A) ^{1}H NMR of **P1** (top) and **P1-ion-S** (bottom) were taken in $C_2D_2Cl_4$ at 110 °C. (B) DSC curves displaying T_m values of LLDPE, **P1**, and **P1-ion-S**. All DSC data were taken from the second heating cycle at a rate of 10 °C/min.

https://doi.org/10.1021/acs.macromol.3c01610
Macromolecules 2023, 56, 8920−8927

significant decrease in the crystallinity percent of the materials. As shown in Figure S6 and Table S3, increasing the degree of functionalization for both pyridyl- and pyridinium-functionalized LLDPE leads to further decreases in crystallinity and melting temperature of the respective materials.

Hierarchical Microphase Separation of Polyolefin Ionomers. An understanding of the impacts of polymer functionalization on the morphological nano- and microstructure of the pyridinium ionomers was obtained through wide-angle X-ray scattering (WAXS) and small-angle X-ray scattering (SAXS). Static WAXS and SAXS scans of unfunctionalized LLDPE as well as pyridyl- and pyridinium-functionalized LLDPE ionomers (1.3 mol % functionalization) in the semicrystalline state (25 °C) are shown in Figures 5, S12, and S13. All WAXS spectra show two primary scattering peaks at wave vector q values of 1.5 $Å^{-1}$ and 1.7 $Å^{-1}$, which correspond to the (110) and (200) reflections of the orthorhombic crystal lattice due to the regular packing of polyethylene chains to form lamellae (Figure 5A). These peaks do not considerably shift in the WAXS spectrum upon functionalization, suggesting that the polyethylene lamellar crystal structure is not altered by the introduction of heteroaryl or charged functional groups and that those groups are likely localized in the amorphous phase of the semicrystalline polymer. To calculate the relative content of the distinct crystalline phases and the overall crystallinity, the integration of the crystalline and amorphous phases reveals that the overall crystallinity diminishes as the degree of functionalization increases, which supports the DSC data (Table S3).

According to the theory of Eisenberg and co-workers for random ionomers on hydrophobic polymer backbones, the ionic groups phase separate into multiplet ion-rich phases that act as physical cross-links within the material.[18] We see evidence of multiplet phases in room-temperature SAXS spectra. Unfunctionalized LLDPE and **P1** show a broad lamellae long-period peak at low scattering vector q of 0.04 $Å^{-1}$, corresponding to a distance of 15.7 nm that is characteristic of the long period of semicrystalline polyethylene (Figure 5B). In contrast, the ionomer **P1-ion-S** has the same isotropic scattering peak as LLDPE along with an additional scattering feature at q of ca. 0.15 $Å^{-1}$, which is equivalent to a distance of ca. 4.2 nm. Based on previous work, we hypothesize that this peak corresponds to the average distance between ionic multiplets dispersed in the amorphous region of LLDPE.[42−45] As the percent functionalization increases, the intensity of the long-period lamellae peak decreases, which is consistent with lower crystallinity observed in WAXS. In contrast, increasing the ionic content from **P1-*ion*-S** to **P3-*ion*-S** results in a shift to higher q of the ionic multiplet peak (i.e., smaller distance) (Figure S13). Temperature-dependent SAXS of **P1-*ion*-S** was also conducted through the melting point of the LLDPE phase, which showed the melting of the polyolefin crystalline phase above 110 °C. In contrast, the scattering peak corresponding to the phase separation of ionic multiplets persisted above the melt temperature of the ionomer (Figure S14). Overall, the X-ray scattering observations confirm a hierarchical assembly of polyolefin ionomers, where lamellar polyethylene crystallites are separated by amorphous domains of polyethylene, within which ion-rich domains phase separate into multiplets (Figure 5C).

Mechanical Properties. We wanted to understand how the hierarchical assembly of the pyridinium ionomers influences the mechanical properties of the materials. Ionic

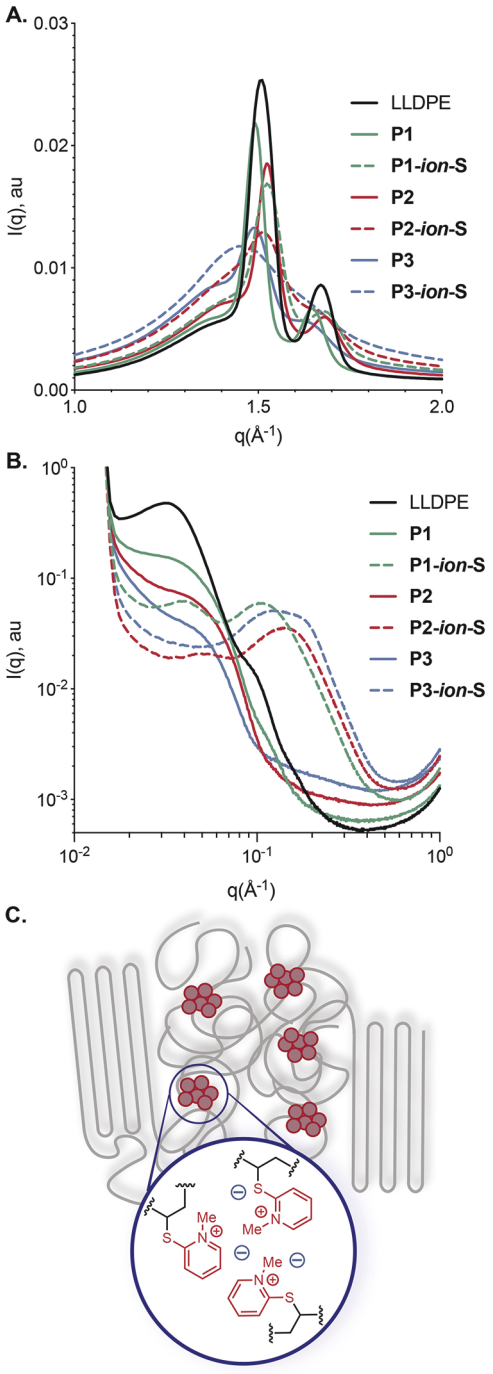

Figure 5. Microphase separation of pyridinium polyolefin ionomers. (A) WAXS spectra demonstrating the reflections corresponding to polyethylene crystallization, which decrease in intensity as functionalization increases. (B) SAXS profiles of LLDPE, **P1**, and **P1-*ion*-S** measured at ambient temperature, wherein the ionomers display an additional scattering peak corresponding to the distance between ionic multiplets. (C) Proposed structure of the cationic ionomer based on the scattering data.

multiplets are known to act as physical cross-links in the polymer melt and impact the viscoelastic properties of the material, which we analyzed through small-amplitude dynamic oscillatory rheological measurements. A strain sweep at a constant frequency (ω) of 1.0 Hz at 130 °C indicated the linear viscoelastic regime LLDPE, **P1**, and **P1-*ion*-S** within a strain range of 1−50% (Figure S15). Subsequently, frequency

https://doi.org/10.1021/acs.macromol.3c01610
Macromolecules 2023, 56, 8920−8927

sweeps for the three materials at a constant strain of 4.0% demonstrated that LLDPE and **P1** exhibit viscous flow at 130 °C corresponding to the terminal region at $\omega < 10$ *rad/s*, where $G' \sim \omega^2$ and $G'' \sim \omega$ (Figure 6). Additionally, the loss

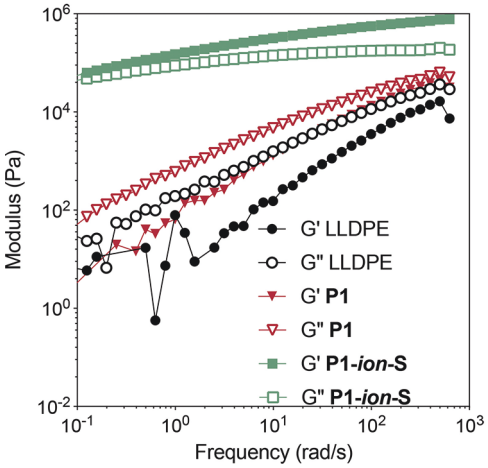

Figure 6. Rheological measurements of the dynamic moduli of LLDPE, **P1**, and **P1-*ion*-S** at 130 °C and 4% strain as a function of frequency, demonstrating that polyolefin ionomers are elastic solids above their T_m due to microphase separation.

and storage moduli of **P1** were higher than those of LLDPE across all frequencies, indicating that the polar thiopyridine groups enhanced interchain interactions and thus increased melt strength. The introduction of ionic groups in **P1-*ion*-S**, however, changed the high-temperature flow characteristics considerably. In this pyridinium ionomer, the moduli increase substantially and G' is larger than G'' across the studied frequency range, indicating that the cross-linking provided by the ionic multiplets imbues the material with solid-like behavior even above the melting temperature of polyethylene. The storage modulus of **P1-*ion*-S** decreases approximately an order of magnitude over the measured frequency range, indicating that ionic multiplets act as dynamic cross-links, whose strength is dependent on the rate of deformation.

The room-temperature mechanical properties of polyolefin ionomers arise from the synergy between two types of noncovalent cross-linking interactions—crystallization and phase separation—which may promote the formation of percolated pathways through the amorphous phase at ambient temperatures.[46] To understand the impact of pyridinium incorporation on the deformation behavior, we exposed thin films of the functionalized polyolefins to uniaxial extension. The stress−strain curve of unfunctionalized LLDPE (Figure 7) demonstrates the tensile response expected for semicrystalline thermoplastics, with high yield stress at low strain, followed by necking of the material until failure. Functionalization of LLDPE with a pyridyl group (**P1**) results in a decrease by approximately half in yield stress and an increase in ductility to >700% elongation at break. The change in behavior is ascribed to the lower degree of crystallinity and concurrent increase in dipole−dipole interchain interactions that promote ductility. Increasing the areal density of pyridyl groups (**P2** and **P3**) results in a similar trend, with a decrease in yield stress and an increase in elongation at break (Figure S18).

Transforming the pyridyl-functionalized LLDPE into a polyolefin ionomer results in ionic multiplets that phase

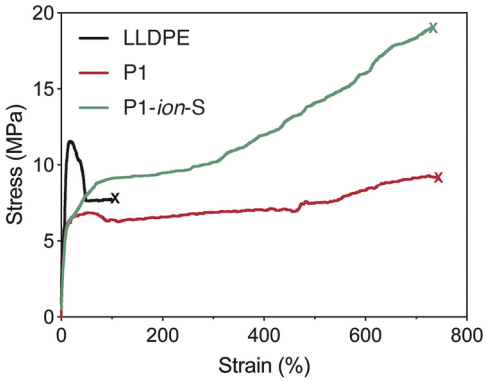

Polymer	σ_B (MPa)	ε_B	U_T (MPa)
LLDPE	8.3 ± 0.9	97 ± 16 %	10.4 ± 2.4
P1	9.3 ± 0.7	793 ± 82 %	56.0 ± 9.7
P1-*ion*-S	19.0 ± 0.3	729 ± 15 %	89.8 ± 2.3

Figure 7. Stress−strain curves for LLDPE, **P1**, and **P1-ion-S** demonstrate the enhanced tensile toughness provided by ionic multiplets. Representative stress−strain curves are shown with averages and standard deviations. Dogbones were pulled at a rate of 0.005 min^{-1}.

separate within the amorphous domains and toughen the material by acting as reversible cross-links that dissociate−reassociate upon deformation.[47] The consequence of these multiplets is a significant increase in the strain stiffening of the material after its initial yield. For the **P1-*ion*-S** material, this results in an increase in tensile toughness (U_T) of ca. nine times compared to LLDPE and almost double compared to the pyridine-functionalized LLDPE. As the mol % of ionic group increases (i.e., ionomers **P2-*ion*-S** and **P3-*ion*-S**), the tensile properties do not change considerably, which is evidenced by the U_T of all ionomers being statistically insignificant from each other (Table S4). These results indicate that the addition of even a small quantity of ionic functionality can lead to significant and potentially beneficial property changes when added to a polyolefin substrate via C−H functionalization.

CONCLUSIONS

A selective and versatile C−H functionalization method is demonstrated that enables the synthesis of polyolefin pyridinium ionomers via C−H bond thioheteroarylation and subsequent ionization. Amidyl radical-mediated C−H functionalization in solution or via reactive extrusion enabled the selective placement of diverse heteroaryl functionalities onto linear and branched polyolefin substrates, including postconsumer plastic waste. The areal density of thiopyridine groups could be systematically varied by altering the stoichiometry of the amide reagent and radical trap during functionalization reactions, and a variety of electrophilic methylating reagents provided efficient access to pyridinium polyolefin ionomers. Temperature-dependent X-ray scattering supported the hypothesis that ionic groups phase separate into ionic multiplets that reside within the amorphous domains of the polyolefin material. Structure−property studies revealed that the ionic multiplets act as physical cross-links both above and below the melting temperature of the polyolefin substrate, which transforms polyolefins into tough thermoplastics upon C−H functionalization. We envision that the ability to synthesize high-value materials from commodity polymers and plastic waste within the common polymer processing

https://doi.org/10.1021/acs.macromol.3c01610
Macromolecules 2023, 56, 8920−8927

infrastructure will expand options for upcycling plastic waste within a more sustainable plastic economy.

■ ASSOCIATED CONTENT

Supporting Information

The Supporting Information is available free of charge at https://pubs.acs.org/doi/10.1021/acs.macromol.3c01610.

General methods and materials, instrumentation, synthesis, experimental information, characterization, and additional spectra (PDF)

■ AUTHOR INFORMATION

Corresponding Author

Frank A. Leibfarth − *Department of Chemistry, The University of North Carolina at Chapel Hill, Chapel Hill, North Carolina 27599, United States;* orcid.org/0000-0001-7737-0331; Email: FrankL@email.unc.edu

Authors

Quan H. Tran − *Department of Chemistry, The University of North Carolina at Chapel Hill, Chapel Hill, North Carolina 27599, United States;* orcid.org/0000-0002-7269-3163

Eliza K. Neidhart − *Department of Chemistry, The University of North Carolina at Chapel Hill, Chapel Hill, North Carolina 27599, United States;* orcid.org/0000-0001-7663-7268

Sergei S. Sheiko − *Department of Chemistry, The University of North Carolina at Chapel Hill, Chapel Hill, North Carolina 27599, United States;* orcid.org/0000-0003-3672-1611

Wim Bras − *Chemical Sciences Division, Oak Ridge National Laboratory, Oak Ridge, Tennessee 37831, United States;* orcid.org/0000-0001-5070-4039

Complete contact information is available at: https://pubs.acs.org/10.1021/acs.macromol.3c01610

Funding

This work was supported by Air Force Office of Scientific Research under Award Number 22RT0214. Scattering experiment was supported by the US Department of Energy, Office of Science, Basic Energy Sciences, Materials Sciences and Engineering Division (FWP# ERKCK60). Rheological and mechanical property testing and expertise provided by S.S.S, funded by the National Science Foundation (DMR 1921835 and DMR 2004048). The UNC Department of Chemistry's NMR Core Laboratory provided expertise and instrumentation that enabled this study with support from National Science Foundation (CHE-1828183 and CHE- 0922858).

Notes

The authors declare the following competing financial interest(s): F.A.L. is an inventor on a U.S. patent application 63/188,215 submitted by UNC Chapel Hill that covers the amide reagents and their use in polymer functionalization.

■ ACKNOWLEDGMENTS

The authors would like to thank Dr. Jong K. Keum (Center for Nanophase Materials Sciences and Neutron Scattering Division, Oak Ridge National Laboratory, Oak Ridge, TN 37830, USA). This research used the resources of the Center for Nanophase Materials Sciences (CNMS) and Spallation Neutron Source (SNS), which are DOE Office of Science User Facilities. WB's contribution is based upon work supported by Oak Ridge National Laboratory, managed by UT-Battelle LLC, for the US Department of Energy. They thank the group of Prof. Theo Dingemans for use of polymer characterization equipment.

■ REFERENCES

(1) Plastics Europe. *Plastics - the Facts*, 2022.

(2) Peacock, A. *Handbook of Polyethylene: Structures, Properties and Applications*; CRC Press: New York, 2000.

(3) Chu, M.; Tu, W.; Yang, S.; Zhang, C.; Li, Q.; Zhang, Q.; Chen, J. Sustainable Chemical Upcycling of Waste Polyolefins by Heterogeneous Catalysis. *SusMat* **2022**, *2* (2), 161−185.

(4) Huang, Z.; Shanmugam, M.; Liu, Z.; Brookfield, A.; Bennett, E. L.; Guan, R.; Vega Herrera, D. E.; Lopez-Sanchez, J. A.; Slater, A. G.; McInnes, E. J. L.; Qi, X.; Xiao, J. Chemical Recycling of Polystyrene to Valuable Chemicals via Selective Acid-Catalyzed Aerobic Oxidation under Visible Light. *J. Am. Chem. Soc.* **2022**, *144* (14), 6532−6542.

(5) Jehanno, C.; Alty, J. W.; Roosen, M.; De Meester, S.; Dove, A. P.; Chen, E. Y.-X.; Leibfarth, F. A.; Sardon, H. Critical Advances and Future Opportunities in Upcycling Commodity Polymers. *Nature* **2022**, *603* (7903), 803−814.

(6) Rahimi, A.; García, J. M. Chemical Recycling of Waste Plastics for New Materials Production. *Nat. Rev. Chem.* **2017**, *1* (6), 0046.

(7) Yin, S.; Tuladhar, R.; Shi, F.; Shanks, R. A.; Combe, M.; Collister, T. Mechanical Reprocessing of Polyolefin Waste: A Review. *Polym. Eng. Sci.* **2015**, *55* (12), 2899−2909.

(8) Hou, Q.; Zhen, M.; Qian, H.; Nie, Y.; Bai, X.; Xia, T.; Laiq Ur Rehman, M.; Li, Q.; Ju, M. Upcycling and Catalytic Degradation of Plastic Wastes. *Cell Rep. Phys. Sci.* **2021**, *2* (8), No. 100514.

(9) Balu, R.; Dutta, N. K.; Choudhury, C. Plastic Waste Upcycling: A Sustainable Solution for Waste Management, Product Development, and Circular Economy. *Polymers* **2022**, *14*, 4788.

(10) Boaen, N. K.; Hillmyer, M. A. Post-Polymerization Functionalization of Polyolefins. *Chem. Soc. Rev.* **2005**, *34* (3), 267−275.

(11) Zhang, Y.; Pedersen, J. N.; Eser, B. E.; Guo, Z. Biodegradation of Polyethylene and Polystyrene: From Microbial Deterioration to Enzyme Discovery. *Biotechnol. Adv.* **2022**, *60*, No. 107991.

(12) Grady, B. P. Review and Critical Analysis of the Morphology of Random Ionomers across Many Length Scales. *Polym. Eng. Sci.* **2008**, *48* (6), 1029−1051.

(13) Bazuin, C. G.; Eisenberg, A. Ion Containing Polymers: Ionomers. *J. Chem. Educ.* **1981**, *58* (11), 938.

(14) Eisenberg, A.; Kim, J.-S. *Introduction to Ionomers*; John Wiley & Sons, Inc.: New York, 1998.

(15) Buitrago, C. F.; Bolintineanu, D. S.; Seitz, M. E.; Opper, K. L.; Wagener, K. B.; Stevens, M. J.; Frischknecht, A. L.; Winey, K. I. Direct Comparisons of X-Ray Scattering and Atomistic Molecular Dynamics Simulations for Precise Acid Copolymers and Ionomers. *Macromolecules* **2015**, *48* (4), 1210−1220.

(16) Mani, S.; Weiss, R. A.; Williams, C. E.; Hahn, S. F. Microstructure of Ionomers Based on Sulfonated Block Copolymers of Polystyrene and Poly(Ethylene-Alt-Propylene). *Macromolecules* **1999**, *32* (11), 3663−3670.

(17) Register, R. A. Morphology and Structure−Property Relationships in Random Ionomers: Two Foundational Articles from Macromolecules. *Macromolecules* **2020**, *53* (5), 1523−1526.

(18) Eisenberg, A.; Hird, B.; Moore, R. B. A New Multiplet-Cluster Model for the Morphology of Random Ionomers. *Macromolecules* **1990**, *23* (18), 4098−4107.

(19) Purgett, M. D.; MacKnight, W. J.; Vogl, O. Functional Polymers LI: Characterization and Property Analysis of ω-Functionally Substituted Polyolefins; Novel Polyolefin Ionomers. *Polym. Eng. Sci.* **1987**, *27* (19), 1461−1468.

(20) Zhang, L.; Brostowitz, N. R.; Cavicchi, K. A.; Weiss, R. A. Perspective: Ionomer Research and Applications. *Macromol. React. Eng.* **2014**, *8* (2), 81−99.

(21) Cavicchi, K. A.; Pantoja, M.; Cakmak, M. Shape Memory Ionomers. *J. Polym. Sci. B: Polym. Phys.* **2016**, *54* (14), 1389−1396.

(22) Norling, P. M. Lessons in New Product Development from DuPont. *Eng. Manage. J.* **1998**, *10* (3), 6−10.
(23) *Structure and Properties of Ionomers*; Pineri, M.; Eisenberg, A., Eds.; Springer: Dordrecht, 1987.
(24) *Ionomers: Synthesis, Structure, Properties, and Applications*; Tant, M. R.; Mauritz, K. A.; Wilkes, G. L., Eds.; Chapman & Hall: New York, 1997.
(25) Zhang, M.; Kim, H. K.; Chalkova, E.; Mark, F.; Lvov, S. N.; Chung, T. C. M. New Polyethylene Based Anion Exchange Membranes (PE−AEMs) with High Ionic Conductivity. *Macromolecules* **2011**, *44* (15), 5937−5946.
(26) Zhang, M.; Yuan, X.; Wang, L.; Chung, T. C. M.; Huang, T.; deGroot, W. Synthesis and Characterization of Well-Controlled Isotactic Polypropylene Ionomers Containing Ammonium Ion Groups. *Macromolecules* **2014**, *47* (2), 571−581.
(27) López-Barrón, C. R.; Lambic, N. S.; Throckmorton, J. A.; Schaefer, J. J.; Smith, A.; Raushel, F. N.; Lin, T.-P. One-Pot Synthesis of High-Melt-Strength Isotactic Polypropylene Ionomers. *Macromolecules* **2022**, *55* (1), 284−296.
(28) Embabi, M.; Kweon, M. S.; Wang, Y. X.; Lin, T.-P.; López-Barrón, C. R.; Lee, P. C. Foaming Performance of Linear Polypropylene Ionomers. *Macromolecules* **2022**, *55* (13), 5645−5655.
(29) Xiang, P.; Ye, Z. Hyperbranched Polyethylene Ionomers Containing Cationic Tetralkylammonium Ions Synthesized by Pd−Diimine-Catalyzed Direct Ethylene Copolymerization with Ionic Liquid Comonomers. *Macromolecules* **2015**, *48* (17), 6096−6107.
(30) Baughman, T. W.; Chan, C. D.; Winey, K. I.; Wagener, K. B. Synthesis and Morphology of Well-Defined Poly(Ethylene-Co-Acrylic Acid) Copolymers. *Macromolecules* **2007**, *40* (18), 6564−6571.
(31) Aitken, B. S.; Lee, M.; Hunley, M. T.; Gibson, H. W.; Wagener, K. B. Synthesis of Precision Ionic Polyolefins Derived from Ionic Liquids. *Macromolecules* **2010**, *43* (4), 1699−1701.
(32) Seitz, M. E.; Chan, C. D.; Opper, K. L.; Baughman, T. W.; Wagener, K. B.; Winey, K. I. Nanoscale Morphology in Precisely Sequenced Poly(Ethylene-Co-Acrylic Acid) Zinc Ionomers. *J. Am. Chem. Soc.* **2010**, *132* (23), 8165−8174.
(33) Aitken, B. S.; Buitrago, C. F.; Heffley, J. D.; Lee, M.; Gibson, H. W.; Winey, K. I.; Wagener, K. B. Precision Ionomers: Synthesis and Thermal/Mechanical Characterization. *Macromolecules* **2012**, *45* (2), 681−687.
(34) Li, Y.; Yao, Z.; Chen, Z.; Qiu, S.; Zeng, C.; Cao, K. High Melt Strength Polypropylene by Ionic Modification: Preparation, Rheological Properties and Foaming Behaviors. *Polymer* **2015**, *70*, 207−214.
(35) Lee, J. A.; Kontopoulou, M.; Parent, J. S. Synthesis and Characterization of Polyethylene-Based Ionomer Nanocomposites. *Polymer* **2005**, *46* (14), 5040−5049.
(36) Yu, J.; He, J. Crystallization Kinetics of Maleic Anhydride Grafted Polypropylene Ionomers. *Polymer* **2000**, *41* (3), 891−898.
(37) Williamson, J. B.; Lewis, S. E.; Johnson, R. R., III; Manning, I. M.; Leibfarth, F. A. C−H Functionalization of Commodity Polymers. *Angew. Chem., Int. Ed.* **2019**, *58* (26), 8654−8668.
(38) Fazekas, T. J.; Alty, J. W.; Neidhart, E. K.; Miller, A. S.; Leibfarth, F. A.; Alexanian, E. J. Diversification of Aliphatic C−H Bonds in Small Molecules and Polyolefins through Radical Chain Transfer. *Science* **2022**, *375* (6580), 545−550.
(39) St Denis, J. D.; He, Z.; Yudin, A. K. Amphoteric α-Boryl Aldehyde Linchpins in the Synthesis of Heterocycles. *ACS Catal.* **2015**, *5* (9), 5373−5379.
(40) Smith, A. B.; Pitram, S. M.; Boldi, A. M.; Gaunt, M. J.; Sfouggatakis, C.; Moser, W. H. Multicomponent Linchpin Couplings. Reaction of Dithiane Anions with Terminal Epoxides, Epichlorohydrin, and Vinyl Epoxides: Efficient, Rapid, and Stereocontrolled Assembly of Advanced Fragments for Complex Molecule Synthesis. *J. Am. Chem. Soc.* **2003**, *125* (47), 14435−14445.
(41) Williamson, J. B.; Na, C. G.; Johnson, R. R.; Daniel, W. F. M.; Alexanian, E. J.; Leibfarth, F. A. Chemo- and Regioselective Functionalization of Isotactic Polypropylene: A Mechanistic and Structure−Property Study. *J. Am. Chem. Soc.* **2019**, *141* (32), 12815−12823.
(42) Eisenberg, A. Clustering of Ions in Organic Polymers. A Theoretical Approach. *Macromolecules* **1970**, *3* (2), 147−154.
(43) Yarusso, D. J.; Cooper, S. L. Microstructure of Ionomers: Interpretation of Small-Angle x-Ray Scattering Data. *Macromolecules* **1983**, *16* (12), 1871−1880.
(44) Benetatos, N. M.; Heiney, P. A.; Winey, K. I. Reconciling STEM and X-Ray Scattering Data from a Poly(Styrene-Ran-Methacrylic Acid) Ionomer: Ionic Aggregate Size. *Macromolecules* **2006**, *39* (16), 5174−5176.
(45) Quiram, D. J.; Register, R. A.; Ryan, A. J. Crystallization and Ionic Associations in Semicrystalline Ionomers. *Macromolecules* **1998**, *31* (4), 1432−1435.
(46) Wakabayashi, K.; Register, R. A. Morphological Origin of the Multistep Relaxation Behavior in Semicrystalline Ethylene/Methacrylic Acid Ionomers. *Macromolecules* **2006**, *39* (3), 1079−1086.
(47) Miwa, Y.; Kurachi, J.; Kohbara, Y.; Kutsumizu, S. Dynamic Ionic Crosslinks Enable High Strength and Ultrastretchability in a Single Elastomer. *Commun. Chem.* **2018**, *1* (1), 6026−6039.

https://doi.org/10.1021/acs.macromol.3c01610
Macromolecules 2023, 56, 8920−8927